Special Feature: Innovative Technologies for the Automotive Structure and Processing

Research Report

Assessment of Hydrogen Absorption and Delayed Fracture Limit of High Tensile Steel Sheet in Corrosive Environment

Gaku Kitahara, Aya Tsuji, Takashi Asada and Tomohiro Suzuki

Report received on Oct. 17, 2019

ABSTRACT For a high tensile steel sheet with a tensile strength above 1200 MPa, it is necessary to properly assess the delayed fracture susceptibility caused by the absorbed hydrogen from corrosive environments. In this study, we proposed an evaluation technique for delayed fracture susceptibility and clarified the effects of the applied stress and the surface treatment on hydrogen absorption for a high tensile steel sheet. Delayed fracture susceptibility can be evaluated based on a delayed fracture limit diagram obtained by the slow strain rate test under cathodic hydrogen charging. We revealed that the application of stress and sacrificial dissolution with a less noble metal than high tensile steel significantly affects the diffusible hydrogen content in the steel. Therefore, it is necessary to consider the effects of the applied stress and the surface treatment when evaluating the diffusible hydrogen absorbed in a car usage environment. The occurrence of the delayed fracture can be determined by comparing the amount of diffusible hydrogen obtained from the applied stress and the surface treatment and the delayed fracture limit diagram.

KEYWORDS Delayed Fracture, Hydrogen Absorption, High Tensile Steel Sheet, Surface Treatment, Stress, Diffusible Hydrogen, Delayed Fracture Susceptibility Evaluation

1. Introduction

The requirements for high tensile steel have increased due to demand for reduced car weight to enhance energy efficiency. However, with increasing strength, the susceptibility of steel to delayed fracture increases.[1] Several techniques have been proposed for evaluating the delayed fracture susceptibility of steel using a round bar specimen with a circumferential notch cathodically charged with hydrogen or immersed in an ammonium thiocyanate solution, including the conventional strain rate test (CSRT),[2-7] the slow strain rate test (SSRT),[6-10] and the constant load test (CLT).[6,7,11-14] It is also necessary to estimate the amount of hydrogen absorbed into steel in a car usage environment. The hydrogen absorption behavior of steel can be evaluated using an electrochemical hydrogen permeation test[15-17] in the ambient atmosphere[18,19] or a corrosive environment.[20-23] Most high tensile steel sheets for car body frames are surface-treated and used in stress-loaded environments. There have been few reports on the delayed fracture susceptibility evaluation of high tensile steel sheets or the effects of surface treatment and applied stress on the absorbed hydrogen content in steel during the corrosion of iron. Because high-strength components in vehicles are used in corrosive environments, it is important to evaluate them. In this study, we propose an evaluation technique for delayed fracture susceptibility and investigate the effects of applied stress and surface treatment on hydrogen absorption for a high tensile steel sheet.

2. Experimental Procedure

2. 1 Delayed Fracture Susceptibility Evaluation of High Tensile Steel Sheet

The CLT and SSRT were used to evaluate the delayed fracture susceptibility. A diagram of the setup for the CLT and SSRT is shown in **Fig. 1**. The material used in this work was a commercial-grade 1500-MPa high tensile steel sheet (see **Fig. 2** for nominal stress-strain curve and **Table 1** for chemical composition). The specimen geometry for the CLT and SSRT is shown in **Fig. 3**. The CLT and SSRT were carried out under cathodic hydrogen charging. The diffusible hydrogen content was controlled by changing the test solution and current density. Cathodic hydrogen charging was

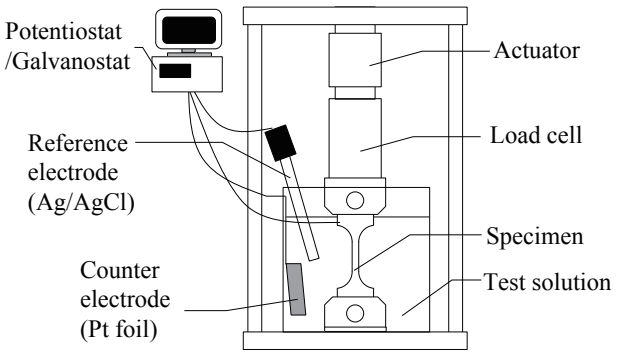

Fig. 1 Schematic diagram of setup for SSRT and CLT.

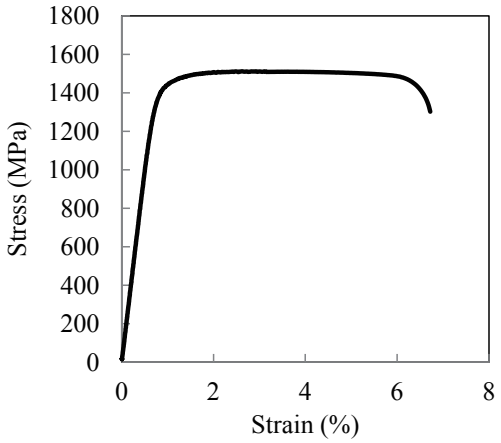

Fig. 2 Nominal stress-strain curve.

Table 1 Chemical composition (mass%) of high tensile steel used in this study.

C	Mn	Si	P	S	Cr	Al	Ti	Nb	V
0.17	1.58	0.49	0.010	0.002	0.03	0.042	0.005	0.013	0.008

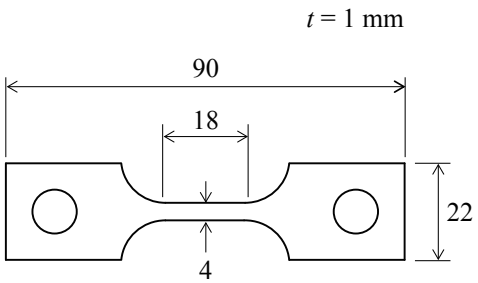

Fig. 3 Specimen used for SSRT and CLT.

conducted using various cathodic charging current densities (0.2-10 mA/cm^2) and ammonium thiocyanate concentrations (NH_4SCN: 0-30 g/L) in an aqueous solution of 3 mass% NaCl with NH_4SCN or 0.1 mol/L NaOH solution.

In the CLT, the loading stress was set to the maximum tensile stress measured without hydrogen (1510 MPa). The ratio of the applied stress to the maximum tensile stress was 0.1-0.92. The CLT was ended when no fracture occurred within 200 h after loading.

The SSRT was conducted at a crosshead displacement rate of 0.005 mm/min (strain rate: 1×10^{-6}/s). Cathodic hydrogen charging for 24 h was conducted prior to the SSRT to homogenize the hydrogen distribution in the specimens.

After testing, the diffusible hydrogen concentration at the reduced section of the specimen near the fracture surface was measured using thermal desorption spectroscopy (TDS) with gas chromatography (SGHA-P2, FIS) or quadrupole mass spectrometry (IH-TDS1700, Denshi-Kagaku Instruments).

2. 2 Evaluation of Diffusible Hydrogen Content in High Tensile Steel Sheet under CLT in Corrosive Environment

To evaluate the effects of applied stress on the diffusible hydrogen content in the specimen, the CLT was carried out in a corrosive environment. The CLT setup was the same as that described in Sec. 2. 1. The specimen geometry is shown in **Fig. 4**. To create a corrosive environment, the specimen was immersed in a test solution containing 3% NaCl solution, with the pH adjusted to 2 by the addition of HCl. The ratio of the applied stress to the maximum tensile stress

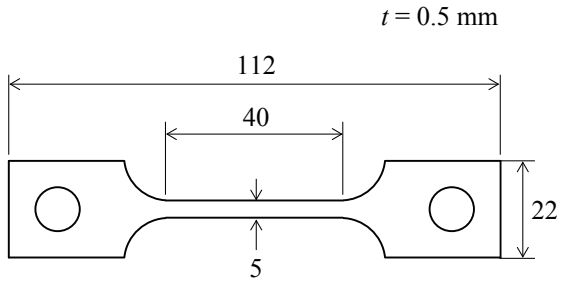

Fig. 4 Specimen used for evaluation of hydrogen absorption under applied load in corrosive environment.

(1510 MPa) was 0.5 (elastic region), 0.90, and 0.92 (plastic region). The duration of the test was 28.8 ks.

After testing, the diffusible hydrogen concentration at the reduced section of the specimen was measured using TDS with quadrupole mass spectrometry (IH-TDS1700, Denshi-Kagaku Instruments).

2. 3 Hydrogen Permeation Measurements of Iron and Iron-zinc Galvanic Couple in Corrosive Environments

Hydrogen permeation tests were conducted using the cells shown in **Figs. 5** and **6** to evaluate the amount of hydrogen absorbed, which is related to the diffusible hydrogen content, during the corrosion of iron and a iron-zinc galvanic couple, respectively. Iron sheets (Nilaco; thickness: 0.2 mm; purity: 99.5%) deposited on a 100-nm-thick nickel layer on the hydrogen detection side of the samples were used in this test. The hydrogen-detection-side chamber was filled with 0.1 mol/L NaOH solution and a potential of +0.15 V vs. Hg/HgO was applied to measure the hydrogen permeation current density, j_H, which is related to the amount of hydrogen absorbed. The hydrogen-entry-side chamber contained an Ag/AgCl reference electrode in saturated KCl (Ag/AgCl) and the test solution for the evaluation of the amount of hydrogen absorbed during the corrosion of iron. For the evaluation of the amount of hydrogen absorbed during corrosion of the iron-zinc galvanic couple, the hydrogen-entry-side chamber contained an Ag/AgCl reference electrode, the test solution, and a zinc sheet (Nilaco; thickness: 0.6 mm; purity: 99%) counter electrode. The zinc sheet that formed the galvanic couple was placed 10 mm from the sample. One side of the zinc sheet was covered with a rubber sealant and the other side of the zinc sheet, which had an exposed surface area of 6.7 cm^2, was placed facing the sample. The test solution was a 3% NaCl solution adjusted to pH 2–14 with HCl or NaOH. On the hydrogen entry side, the sample was connected to the reference electrode via a potentiostat/galvanostat and the counter electrode via a zero-shunt ammeter to measure the corrosion potential, E_{corr}, and the galvanic current density, j_{gal}, during the corrosion of iron or the sacrificial dissolution of zinc. All immersion corrosion tests were performed for over 30 ks at 25°C.

3. Results and Discussion

3. 1 Delayed Fracture Susceptibility Evaluation of High Tensile Steel Sheet

The relationship between the tensile stress/applied stress obtained from the CLT and SSRT and the diffusible hydrogen content (i.e., the fracture limit

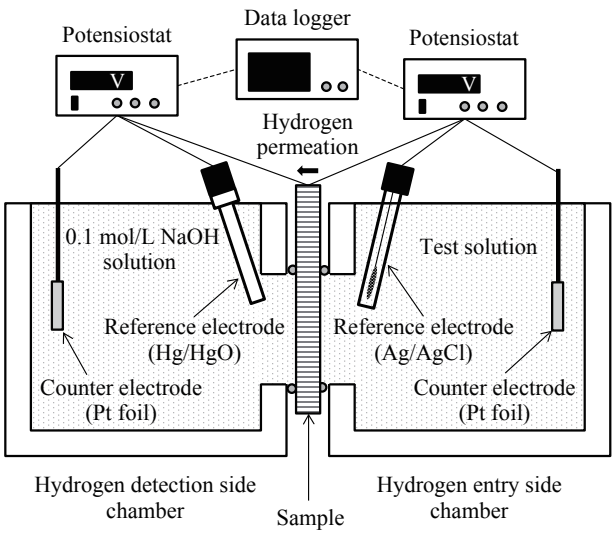

Fig. 5 Schematic diagram of electrochemical cell used to evaluate hydrogen absorption into iron sheet during corrosion of iron in immersion corrosion tests.

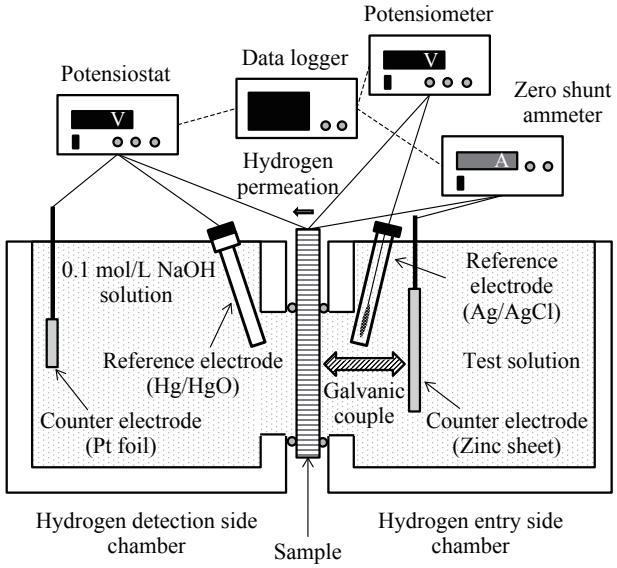

Fig. 6 Schematic diagram of electrochemical cell used to evaluate hydrogen absorption into iron sheet during corrosion of iron-zinc galvanic couple in immersion corrosion tests.

diagram) for the specimens is shown in **Fig. 7**. The white and black triangles indicate unfractured and fractured specimens in the CLT, respectively. The fracture strength was constant until less than 0.5 wt. ppm of diffusible hydrogen. For a diffusible hydrogen content of more than 0.5 wt. ppm, the fracture strength remarkably decreased with increasing hydrogen content. The delayed fracture limit curve obtained from the SSRT for this specimen is the dotted line in the figure. In the CLT, many specimens fractured in the fracture region of the delayed fracture limit diagram of the SSRT. The CLT and SSRT provide similar relationships between the tensile stress and applied stress of fractured specimens and the diffusible hydrogen content because in both methods, there is sufficient time for stress-induced diffusion of hydrogen and interaction between dislocations and hydrogen.

3. 2 Evaluation of Diffusible Hydrogen Content in High Tensile Steel Sheet under Applied Load in Corrosive Environment

Figure 8 shows the TDS spectra obtained for specimens subjected to the CLT under various stress levels (0, 0.5, 0.90, $0.92\sigma_B$) in the immersed corrosion environment. The specimen under no load conditions yielded a small symmetric spectrum with a peak at around 50°C (dotted line in Fig. 8(b)). The test with $0.5\sigma_B$ yielded a similar hydrogen desorption peak around 50°C, but hydrogen desorption continued during further heating to 200°C. For the specimens to which stress was applied to achieve plastic deformation ($0.9\sigma_B$ and $0.92\sigma_B$), intense asymmetric hydrogen desorption spectra with a peak at around 80°C with tailing up to 150°C were obtained. It has been reported that a low-temperature peak that appears in the range of 0 to 50°C can be attributed to hydrogen desorption from trap sites at dislocations and crystal grain boundaries; a peak at around 100°C can be attributed to the desorption of hydrogen trapped at vacancy clusters generated by the applied stress.[24,25] In the TDS spectra in Fig. 8, the low-temperature peak in the range of 50 to 80°C is attributed to the release of hydrogen trapped at dislocations and crystal grain boundaries, and the small peak at around 100°C with a tail to 200°C is attributed to the desorption of hydrogen trapped at vacancy clusters. This implies that the stress applied in the CLT promoted the formation of hydrogen trapping sites, such as dislocations,

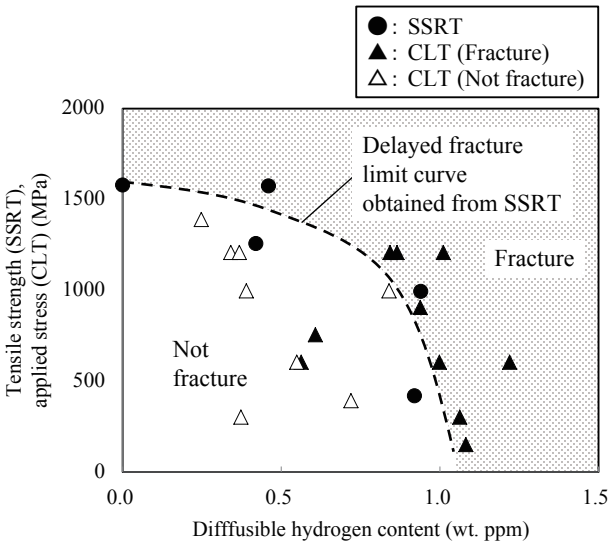

Fig. 7 Diffusible hydrogen content versus tensile strength/applied stress obtained from SSRT and CLT.

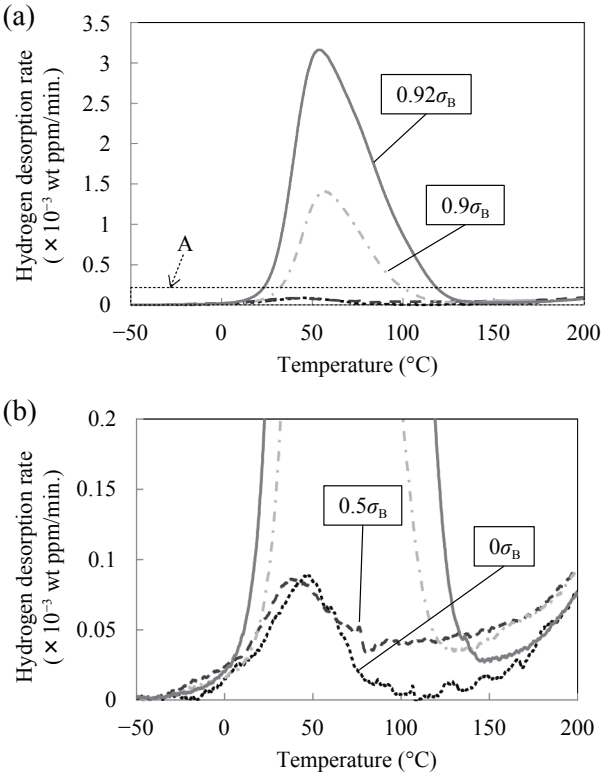

Fig. 8 Hydrogen desorption curves for specimens under various stress levels. (a) General view and (b) enlarged view.

grain boundaries, and vacancy clusters, resulting in an increased amount of diffusible hydrogen trapped in the steel. For a quantitative analysis of diffusible hydrogen content in the steel subjected to the CLT, the TDS peak was analyzed under the assumption that the hydrogen desorption temperature range for peaks attributed to dislocations and grain boundaries was 50 to 80°C and that for vacancy clusters was 90 to 130°C. The analysis was conducted using the pseudo-Voigt function and the least-mean-squares method for peak separation (resolution) and fitting[26] to estimate the amount of trapped diffusible hydrogen for the respective defect sites in the steel from the peak area. **Figure 9** shows an example of TDS peak resolution and fitting for the specimen subjected to the CLT with $0.92\sigma_B$. The detected TDS peak for the specimen was separated into two profiles, namely profile 1 for the contribution from hydrogen desorbed from dislocations and crystal grain boundaries, and profile 2 for hydrogen desorbed from vacancy clusters generated by the applied stress. From the peak resolution and fitting, the total amount of diffusible hydrogen, hydrogen trapped at dislocations and crystal grain boundaries (profile 1), and hydrogen trapped at vacancy clusters (profile 2) were evaluated; the results are plotted in **Fig. 10**. As shown, the diffusible hydrogen trapped at lattice defects increased with increasing applied stress. The increase in the amount of trapped diffusible hydrogen was especially significant when the applied stress caused plastic deformation ($\sigma \geq 0.9\sigma_B$). The diffusible hydrogen content in the steel increased by a factor of a few tens under an applied stress that led to plastic deformation.

3. 3 Hydrogen Permeation Measurements for Iron and Iron-zinc Galvanic Couple in Corrosive Environments

Figure 11 shows the variation in the mean values of $j_{H,\infty}$, E_{corr}, and j_{gal} in the steady state as a function of pH for the corrosion of the iron-zinc galvanic couple (diamonds) and iron (without zinc) (triangles). The surface hydrogen concentration, which is related to the diffusible hydrogen content, can be calculated from the values of $j_{H,\infty}$ in the steady state. j_{gal} is related to the corrosion rate of zinc and hydrogen evolution from iron under zinc sacrificial dissolution.

The increase of $j_{H,\infty}$ for the iron-zinc galvanic couple was larger than that for iron at all tested pH values. This suggests that hydrogen absorption was promoted by the formation of the iron-zinc galvanic couple.

The E_{corr} value for iron (without zinc) was between −0.6 and −0.7 V in the pH range of 2–12, but increased to −0.2 V at pH 12. For the iron-zinc galvanic couple, the E_{corr} value was below that for iron: −1.0 V in the pH range of 2–12 and −1.4 V at pH 14.

The pH dependence of j_{gal} is a parabolic curve (opening upward). j_{gal} was relatively low in the pH range of 7–12, primarily due to the formation of a protective film of corrosion products on the zinc surface. However, j_{gal} increased considerably on either side in the pH range of 7–12 because zinc is an amphoteric metal and dissolves readily in acidic or strongly alkaline solutions. The pH dependence of j_{gal} is similar to that for the zinc corrosion rate described in previous reports.[27-29]

For iron, $j_{H,\infty}$ decreased with increasing pH. Hydrogen evolution reactions have occurred mainly

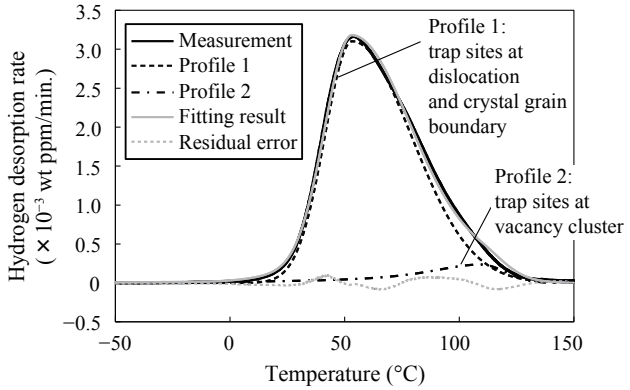

Fig. 9 Example of peak resolution of hydrogen desorption curve for $0.92\sigma_B$.

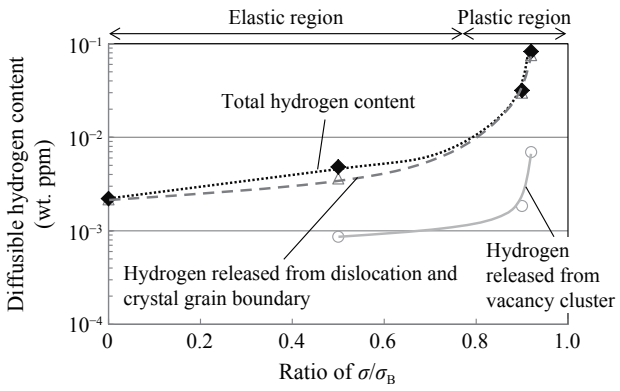

Fig. 10 Diffusible hydrogen content versus σ/σ_B ratio.

in acid solutions with pH values below 4, indicating that hydrogen was absorbed at these pH values. As a result, it is assumed that $j_{H,\infty}$ increased in acid solutions with pH values below 4. In the pH range of 4–10, $j_{H,\infty}$ was relatively independent of the solution pH, and the iron corrosion rate was governed largely by the rate of the oxygen reduction reaction, which was constant regardless of pH. For pH values above 10, the corrosion rate decreased with increasing pH. In alkaline solutions with pH above 10, a protective Fe_2O_3 oxide layer formed, and $j_{H,\infty}$ decreased with increasing pH. The layer protected the iron from corrosion and inhibited hydrogen absorption. During the formation of the iron-zinc galvanic couple, the relationship between $j_{H,\infty}$ and pH was approximately the same as that between j_{gal} and pH. This is possibly due to the same reasons for the variation of j_{gal}. Because the hydrogen overpotential is low on the surface of iron, hydrogen evolution occurs at the potential (E_{corr}) at which iron forms a galvanic couple with zinc. Furthermore, hydrogen evolution occurs at the same rate as zinc dissolution at the surface of iron; the hydrogen flux into the iron changes accordingly. As a result, the trends of the changes in $j_{H,\infty}$ and j_{gal} are similar.

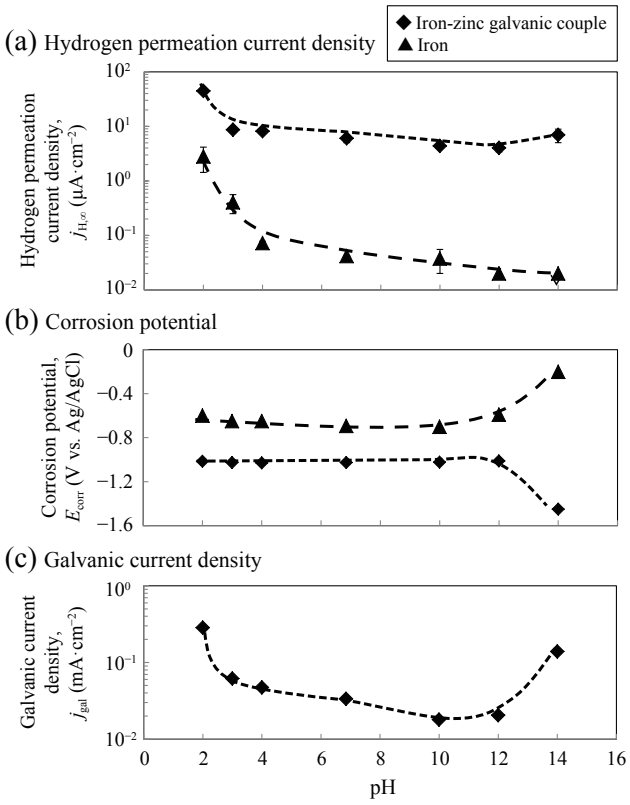

Fig. 11 Mean value variations for $j_{H,\infty}$, E_{corr}, and j_{gal} for iron-zinc galvanic couple (diamonds) and during corrosion of iron without zinc (triangles) with pH in steady state.

4. Delayed Fracture Limit Diagram and Amount of Hydrogen Absorbed

Figure 12 shows the threshold curve obtained from the curve of fracture stress versus diffusible hydrogen content for various conditions. In Sec. 3. 2, we revealed that the diffusible hydrogen content in the steel increased by a factor of a few tens under the application of stress that caused plastic deformation. In Sec. 3. 3, we revealed that the amount of hydrogen absorbed due to zinc sacrificial dissolution was larger than that due to iron corrosion in the entire pH range. Under the combination of applied stress and surface treatment, it is expected that more diffusible hydrogen will be absorbed than under no applied stress and/or surface treatment for the same corrosive environment. Therefore, it is necessary to consider applied stress and surface treatment when evaluating the amount of diffusible hydrogen. The occurrence of delayed fracture can be determined by comparing the amount of diffusible hydrogen obtained from applied stress and surface treatment and the fracture limit diagram.

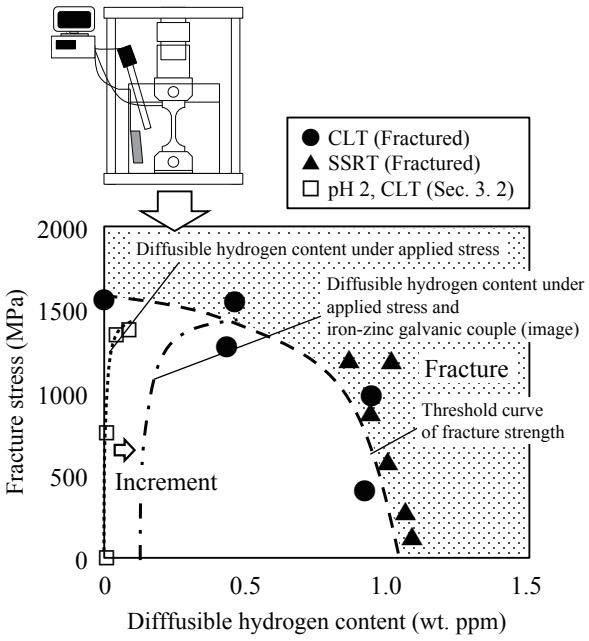

Fig. 12 Fracture stress versus diffusible hydrogen content for various conditions.

5. Conclusions

(1) The CLT and SSRT provide similar relationships between the diffusible hydrogen content and the tensile stress/fracture stress because in both methods, there is sufficient time for stress-induced diffusion of hydrogen and interaction of dislocations and hydrogen.
(2) The diffusible hydrogen content in the steel increased by a factor of a few tens under the application of stress that caused plastic deformation.
(3) The amount of hydrogen absorbed when iron was corroded increased with decreasing solution pH.
(4) The amount of hydrogen absorbed due to zinc sacrificial dissolution was larger than that due to iron corrosion in the entire pH range, and was well-correlated with the rate of zinc dissolution.
(5) Our results imply that the application of stress and sacrificial dissolution with a less noble metal than high tensile steel significantly affect the diffusible hydrogen content in the steel. Therefore, it is necessary to consider the effects of stress and surface treatment when evaluating the amount of hydrogen absorbed in a car usage environment.

Acknowledgments

The authors thank Dr. H. Kobayashi and Dr. K. Horikawa (Osaka University) for discussion and encouragement.

References

(1) Fujita, T. and Yamada, Y., "Physical Metallurgy and SCC in High Strength Steels", *Proc. Stress Corrosion Cracking and Hydrogen Embrittlement of Iron Base Alloys* (1977), pp. 736-746, National Association of Corrosion Engineers.
(2) Hagihara, Y., Ito, C., Hisamori, N., Suzuki, H., Takai, K. and Akiyama, E., "Evaluation of Delayed Fracture Characteristics of High Strength Steel Based on CSRT Method", *Tetsu-to-Hagane* (in Japanese), Vol. 94, No. 6 (2008), pp. 215-221.
(3) Hagihara, Y., Ito, C., Kirikae, D., Hisamori, N., Suzuki, H. and Takai, K., "Probabilistic and Statistical Evaluation of Delayed Fracture Characteristics Obtained by CSRT Method", *Tetsu-to-Hagane* (in Japanese), Vol. 95, No. 6 (2009), pp. 489-497.
(4) Hagihara, Y., Shobu, T., Hisamori, N., Suzuki, H., Takai, K. and Hirai, K., "Delayed Fracture Using CSRT Method and Hydrogen Trapping Characteristics of V-bearing High Strength Steel", *Tetsu-to-Hagane* (in Japanese), Vol. 97, No. 3 (2011), pp. 143-151.
(5) Hojo, T., Waki, H. and Nishimura, F., "Evaluation for Hydrogen Embrittlement Properties of Tempered Martensitic Steel Sheets Using Several Testing Technique", *Tetsu-to-Hagane* (in Japanese), Vol. 100, No. 10 (2014), pp. 1306-1314.
(6) Chida, T., Hagihara, Y., Akiyama, E., Iwanaga, K., Takagi, S., Ohishi, H., Hayakawa, M., Hirakami, D. and Tarui, T., "Comparison of Constant Load, SSRT and CSRT Methods for Hydrogen Embrittlement Evaluation Using Round Bar Specimens of High Strength Steels", *Tetsu-to-Hagane* (in Japanese), Vol. 100, No. 10 (2014), pp. 1298-1305.
(7) Takagi, S., Hagihara, Y., Hojo, T., Urushihara, W. and Kawasaki, K., "Comparison of Hydrogen Embrittlement Resistance of High Strength Steel Sheets Evaluated by Several Methods", *ISIJ Int.*, Vol. 56, No.4 (2016), pp.685-692.
(8) Wang, M., Akiyama, E. and Tsuzaki, K., "Effect of Hydrogen and Stress Concentration on the Notch Tensile Strength of AISI 4135 Steel", *Mater. Sci. Eng., A*, Vol. 398, No. 1-2 (2005), pp. 37-46.
(9) Wang, M., Akiyama, E. and Tsuzaki, K., "Crosshead Speed Dependence of the Notch Tensile Strength of a High Strength Steel in the Presence of Hydrogen", *Scr. Mater.*, Vol. 53, No. 6 (2005), pp. 713-718.
(10) Wang, M., Akiyama, E. and Tsuzaki, K., "Effect of Hydrogen on the Fracture Behavior of High Strength Steel during Slow Strain Rate Test", *Corros. Sci.*, Vol. 49, No.11 (2007), pp. 4081-4097.
(11) Kushida, T., Matsumoto, H., Kuratomi, N., Tsumura, T., Nakasato, F. and Kudo, T., "Delayed Fracture and Hydrogen Absorption of 1.3 GPa Grade High Strength Bolt Steel", *Tetsu-to-Hagane* (in Japanese), Vol. 82, No. 4 (1996), pp. 297-302.

(12) Takagi, S., Hagihara, Y., Hojo, T., Urushihara, W. and Kawasaki, K., "Comparison of Hydrogen Embrittlement Resistance of High Strength Steel Sheets Evaluated by Several Methods", *Tetsu-to-Hagane* (in Japanese), Vol. 100, No. 10 (2014), pp. 1315-1321.
(13) Yamasaki, S. and Takahashi, T., "Evaluation Method of Delayed Fracture Property of High Strength Steels", *Tetsu-to-Hagane* (in Japanese), Vol. 83, No. 7 (1997), pp. 454-459.
(14) Takagi, S., Inoue, T., Hara, T., Hayakawa, M., Tsuzaki, K. and Takahashi, T., "Parameters for the Evaluation of Hydrogen Embrittlement of High Strength Steel", *Tetsu-to-Hagane* (in Japanese), Vol. 86, No. 10 (2000), pp. 689-696.
(15) Devanathan, M. A. V. and Stachurski, Z., "The Adsorption and Diffusion of Electrolytic Hydrogen in Palladium", *Proc. R. Soc. London, Ser. A*, Vol. 270, No. 1340 (1962), pp. 90-102.
(16) Kushida, T., "Hydrogen Entry into Steel by Atmospheric Corrosion" *ISIJ Int.*, Vol. 43, No. 4 (2003), pp. 470-474.
(17) Tsuru, T., "Electrochemical Measurements for Hydrogen Entry and Permeation of Steel", *Zairyo-to-Kankyo* (in Japanese), Vol. 63, No. 1 (2014), pp. 3-9.
(18) Tsuru, T., Huang, Y., Ali, M. R. and Nishikata, A., "Hydrogen Entry into Steel during Atmospheric Corrosion Process", *Corros. Sci.*, Vol. 47, No. 10 (2005), pp. 2431-2440.
(19) Li, S., Akiyama, E., Shinohara, T., Matsuoka, K. and Oshikawa, W., "Hydrogen Entry Behavior into Iron and Steel under Atmospheric Corrosion", *ISIJ Int.*, Vol. 53, No. 6 (2013), pp. 1062-1069.
(20) Turnbull, A., Saenz de Santa Maria, M. and Thomas, N. D., "The Effect of H_2S Concentration and pH on Hydrogen Permeation in AISI 410 Stainless Steel in 5% NaCl", *Corros. Sci.*, Vol. 29, No. 1 (1989), pp. 89-104.
(21) Omura, T., Kushida, T., Kudo, T., Nakasato, F. and Watanabe, S., "Environmental Factors Affecting Hydrogen Absorption into Steels", *Zairyo-to-Kankyo* (in Japanese), Vol. 54, No. 2 (2005), pp. 61-67.
(22) Hara, T. and Tarui, T., "Hydrogen Entry Behavior into Steel in Alkaline Environment", *Zairyo-to-Kankyo* (in Japanese), Vol. 59, No. 5 (2010), pp. 173-178.
(23) Hara, T., "Hydrogen Entry Behavior into Steel in Immersion Environments", *Zairyo-to-Kankyo* (in Japanese), Vol. 60, No. 5 (2011), pp. 259-264.
(24) Takai, K., "Hydrogen Existing States and Hydrogen Embrittlement", *Zairyo-to-Kankyo* (in Japanese), Vol. 60, No. 5 (2011), pp. 230-235.
(25) Takai, K., "Common Bases and Recent Progress on Hydrogen Embrittlement Studies of Steels", *Sanyo Technical Report* (in Japanese), Vol. 22 (2015), pp. 14-20.
(26) Toraya, H., "Profile Functions and the Pattern Decomposition Method", *Nihon Kessho Gakkaishi* (in Japanese), Vol. 34, No. 2 (1992), pp. 86-99.
(27) Della Rovere, C. A., Silva, R., Moretti, C. and Kuri, S. E., "Corrosion Failure Analysis of Galvanized Steel Pipes in a Water Irrigation System", *Eng. Failure Anal.*, Vol. 33 (2013), pp. 381-386.
(28) Roetheli, B. E., Cox, G. L. and Littreal, W. B., "Effect of pH on the Corrosion Products and Corrosion Rate of Zinc in Oxygenated Aqueous Solutions", *Met. Alloys*, Vol. 3 (1932), pp. 73-76.
(29) Thomas, S., Birbilis, N., Venkatraman, M. S. and Cole, I. S., "Corrosion of Zinc as a Function of pH", *Corrosion*, Vol. 68, No. 1 (2012), 015009-1-015009-9.

Gaku Kitahara

Research Fields:
- Electrochemistry
- Surface Treatment (Metal Coating)
- Corrosion
- Hydrogen Embrittlement

Academic Degree: Ph.D.
Academic Societies:
- Japan Society of Corrosion Engineering
- The Japan Institute of Metals and Materials
- The Iron and Steel Institute of Japan

Aya Tsuji

Research Fields:
- Hydrogen Embrittlement
- Mechanical Property Evaluation of Materials

Academic Societies:
- The Japan Society of Mechanical Engineers
- The Iron and Steel Institute of Japan
- The Society of Materials Science, Japan

Takashi Asada

Research Fields:
- Dissimilar Metals Joining
- Hydrogen Embrittlement

Academic Degree: Ph.D.
Academic Society:
- The Japan Society of Mechanical Engineers

Award:
- Young Engineers Award, The Japan Society of Mechanical Engineers, 2016

Tomohiro Suzuki

Research Fields:
- Metallic Materials
- Fatigue and Hydrogen Embrittlement

Academic Degree: Ph.D.
Academic Societies:
- The Japan Society of Mechanical Engineers
- The Society of Materials Science, Japan

Award:
- Young Engineers Award, The Japan Society of Mechanical Engineers, 2001

